A R C H I V E S O F M E T A L L U R G Y A N D M A T E R I A L S
Volume 60 2015 Issue 2
DOI: 10.1515/amm-2015-0151

A. GYENES[*,♯], A. SIMON[**], P. LANSZKI[*], Z. GÁCSI[*]

EFFECTS OF NICKEL ON THE MICROSTRUCTURE AND THE MECHANICAL PROPERTIES OF Sn-0.7Cu LEAD-FREE SOLDERS

WPŁYW NIKLU NA MIKROSTRUKTURĘ I WŁAŚCIWOŚCI MECHANICZNE BEZOŁOWIOWYCH STOPÓW LUTOWNICZYCH Sn-0.7Cu

This paper investigates the effects of small amount nickel addition (0, 200, 400, 800, 1800 ppm) on the microstructure and the mechanical properties of Sn-0.7Cu lead-free solder alloys. It is known that even ppm level Ni additions have significant effects on the microstructure of Sn-Cu solder alloys. Ni suppresses the growth of β-Sn dendrites in favour of eutectic formation. As the nickel content increases, the microstructure undergoes a morphological evolution from hypoeutectic through fully eutectic to hypereutectic. Along with these transformations, the mechanical properties of the alloy also significantly change. Based on the experimental results presented in this paper, the Sn-0.7Cu solder achieves maximum strength at the addition level of 800 ppm Ni, when the microstructure becomes fully eutectic.

Keywords: Sn-0.7Cu, lead-free solder, Ni addition, microstructure, mechanical properties

1. Introduction

Recently, the Directives 2011/65/EU and 2012/19/EU, commonly referred to as RoHS (Restriction of Hazardous Substances) and WEEE (Waste Electrical and Electronic Equipment), were adopted by the European Union out of health and environmental reasons to restrict the use of toxic lead in electrical and electronic equipment and to oblige market participants to produce more environmentally friendly electronic products [1,2]. Therefore, the electronics and automotive industry should switch from traditionally used Sn-Pb solders to Pb-free solders, which entails the continuous development of new alloys. Already in commercial use, the near-eutectic Sn-0.7Cu alloy has become a very promising alternative as lead-free solder for wave soldering applications, mainly due to cost issues [3-5].

According to the phase diagrams reported in the literature, the Sn-Cu system undergoes an eutectic reaction at 227°C [5,6,9]. However, there are differences in the ways the exact eutectic composition is calculated. Moura et al. [5] define the eutectic composition at 0.7 wt.% Cu (by Thermocalc® database), while Nogita and other authors indicate it at 0.89 wt.% Cu [4,7,9]. The eutectic reaction occurs between the faceted eutectic Cu_6Sn_5 phase and the non-faceted Sn-rich phase [9]. The Cu_6Sn_5 phase grows in the form of rods embedded in a continuous Sn-rich matrix [5]. Ventura et al. studied the influence of growth velocity and Cu content on the microstructure of near-eutectic Sn-Cu solder alloys. They found that for relatively high growth velocities and for Cu contents below 0.9 wt.%, the microstructure consists of primary β-Sn cells or dendrites surrounded by eutectic (β-Sn+Cu_6Sn_5)[4,7].

Table 1 summarizes the mechanical properties of Sn-0.7Cu lead-free solders at room temperature, as substracted from the relevant database reported in the literature. Significant differences can be observed in the values of tensile strength (19.4-52.0 MPa), yield stress (15.3-47.8 MPa) and elongation (11.7-72 %), certainly attributable to different specimen preparation processes and test conditions.

It is known that even ppm levels of nickel addition have significant effects on several properties of Sn-Cu alloys. Nickel can improve the soldering properties of Sn-Cu alloys by reducing the tendency for bridging and by enhancing the solder-substrate interface and the surface finish [6]. The effects of Ni on the microstructure of directionally solidified Sn-0.7Cu alloys have been widely investigated [6-8]. A transition from hypoeutectic (primary β-Sn cells or dendrites and eutectic (β-Sn+Cu_6Sn_5)), to fully eutectic and finally hypereutectic (primary $(Cu,Ni)_6Sn_5$ intermetallics and eutectic (β-Sn+$(Cu,Ni)_6Sn_5$)) microstructure was observed with increasing Ni content at 10 μm/s growth rate [6,7]. It was shown that nickel suppresses the formation of β-Sn dendrites and instead promotes the evolution of a fully eutectic microstructure. However, above certain Ni contents (500-1000 ppm, depending on growth velocity), large primary intermetallic phases appear in the microstructure [6].

[*] INSTITUTE OF PHYSICAL METALLURGY, METAL FORMING AND NANOTECHNOLOGY, UNIVERSITY OF MISKOLC, H-3515 MISKOLC-EGYETEMVÁROS, HUNGARY
[**] INSTITUTE OF CERAMICS AND POLYMER ENGINEERING, UNIVERSITY OF MISKOLC, H-3515 MISKOLC-EGYETEMVÁROS, HUNGARY
[♯] Corresponding author: femanett@uni-miskolc.hu

TABLE 1

Mechanical properties of the Sn-0.7Cu solder

UTS [MPa]	YS [MPa]	El [%]	Strain rate [s^{-1}]	Specimen preparation	HV	Ref.
31*	-	72*	5×10^{-3}	cast (Cu mould), cylindrical (Ø5 mm), polished, heat-treated (100°C, 2 h)	14 (10g) 12.4 (50g)	11
37.5	25	25	5×10^{-3}	cast (cooling rate: ~1.5 K/s), cylindrical (Ø5 mm), heat treated (100°C, 2 h) prior to being machined	14.5 (50g)	12
30.5*	26*	15*	3.47×10^{-4}	cast (steel mould), dog-bone, polished, heat-treated (100°C, 30min), average of >8 measurements	-	13
19.4 21.6	15.3 16.0	20.8 41.2	1.3×10^{-4}	cast (preheated titanium mould), cylindrical (Ø 3.8 mm), polished, *water quenched,* *air cooled,* heat-treated (151°C, 16 hours), average of 3 measurements		14
				solder doplet (Cu plate) cooling rate: 32°C/s 8°C/s 5°C/s	10.3* 10.8* 12.5*	14
28.0	20.4	44.0	1.2×10^{-2}	cast (steel mould, cooling rate: 6-8°C/s), cylindrical Ø2.5 mm, heat-treated (130°C, 30min), average of 3 measurements	-	15
22	16.3	39.1	1.8×10^{-3}	cast (steel mould, cooling rate: 6-8°C/s), cylindrical Ø3.5 mm average of 3 measurements		16
20	17	33.6	-	-	-	16
22	15	39	-	-	-	16
35.8 45.0 52.0	31.1 36.5 47.8	- - -	5.6×10^{-4} 5.6×10^{-3} 5.6×10^{-2}	bulk solder, dog-bone, cylindrical (Ø3 mm)		17
29	24	23	3.3×10^{-5}	cast (metallic mould), homogenized (100°C, 24h) prior to machining, cylindrical Ø4.5 mm	-	18
25*	-	11.7*	1×10^{-3}	directionally solidified, average of 4 measurements		19

∗ *The marked values are read from diagrams reported in the study.*

TABLE 2

Mechanical properties of Sn-0.7Cu-xNi alloys

Solder alloy	UTS [MPa]	YS [MPa]	El [%]	Strain rate [s^{-1}]	Specimen preparation	Ref.
Sn-0.7Cu-0.12Ni	34.4* 26.8* 24.2* 20.6*	25* 23* 20* 18*	-	1.20×10^{-2} 1.17×10^{-3} 1.15×10^{-4} 4.01×10^{-5}	cast (steel mould); aged (T_{room}, >2 months); dog-bone, polished, heat-treated (100°C, 60 min)	20
Sn-0.7Cu-0.12Ni	33.3* 28.0* 23.0* 21.8* 19.3*	-	46.4* 40.0* 28.9* 36.4* 46.9*	1×10^{-2} 3×10^{-3} 1×10^{-3} 3×10^{-4} 1×10^{-4}	cylindrical (Ø1.8 mm), heat-treated (193°C, 3h) and aged (T_{room}, >20 days)	21
Sn-0.7Cu-0.05Ni	36.5*	-	6.1*	$1x10^{-3}$	directionally solidified, average of 4 measurements	19
Sn-0.7Cu-0.1Ni	34.4*	-	12.1*			

∗ *The marked values are read from diagrams reported in the study*

Furthermore, it is known that Ni is strongly segregated by Sn and highly soluble in Cu_6Sn_5 forming $(Cu,Ni)_6Sn_5$ phase [7]. The presence of Ni in the intermetallic even at concentrations of about 5 at.% can stabilise the high-temperature η-Cu_6Sn_5 phase over a large temperature range (-100°C-250°C). Therefore, the allotropic transformation of Cu_6Sn_5 phase from monoclinic (η'-Cu_6Sn_5) to hexagonal (η-Cu_6Sn_5) – which normally occurs at 186°C in the Sn-Cu

system – cannot take place. This in turn, prevents volume changes, which would result in internal stresses and finally cracking [9].

Table 2 shows the mechanical properties of Sn-0.7Cu-xNi alloys as given in the literature. Unlike microstructure characterisations, the effects of nickel content on the mechanical properties of Sn-0.7Cu lead-free solders are not fully reported. Only a few studies can be found in this research area [19-21]. Therefore, the purpose of this study is to investigate the modifications triggered by Ni in the microstructure and the mechanical properties of Sn-0.7Cu lead free solders and to set up a correlation between them.

2. Experimental methods

Industrial solder ingots of Sn-0.7Cu were used in the experiments to study commercial purity materials. The tested solder alloy was melted at 400°C in an electric resistance furnace. Different amounts of Ni in the form of SnNi10 master alloy were added to the solder melt. Subsequent to nickel addition and stirring, an incubation time of 30 min was applied to achieve the complete the dissolution of nickel. The alloys were poured into a pre-heated (to 200°C) steel mould of tensile test rods with a diameter of 11 mm. Three samples were casted from each alloy. The chemical compositions of the test samples were analysed by a Varian Inc. 720 -ES type ICP (inductively coupled plasma) spectrometer, the results are listed in Table 3.

Microstructure observations were carried out on the transverse sections of the as-cast samples. The following metallographic process was used:

- grounding – with P240, P320, P500, P800, P1200, P2000, P2400 SiC papers and water;
- polishing – with 3 μm, then 1 μm baize and DP-Lubricant Blue (Struers);
- final polishing – with MasterMet^{TM} 2 (Buehler) non-crystallizing colloidal silica (0.02 μm) polishing suspension.

Microstructure was observed using a Zeiss AxioVision Imager m1M optical microscope and a Hitachi S4800 scanning electron microscope (SEM). The phase compositions of the samples were measured by a Bruker energy dispersive X-ray spectrometer (EDX).

Tensile test specimens were machined from the cast rods according to DIN-EN-50125 standard shown in Fig.1. The tests were performed at room temperature at a strain rate of 10^{-3} s^{-1} (displacement rate: 3 mm/min) by an Instron 5982 type universal testing machine. The mechanical properties of the samples were obtained by averaging each 3 test data.

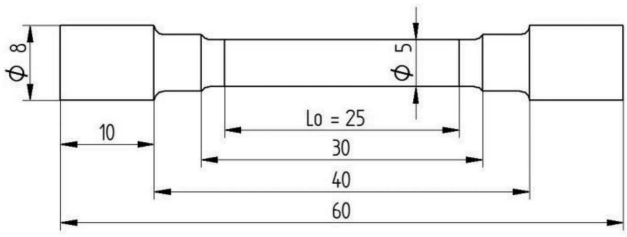

Fig. 1. Scheme of tensile test specimen

Microhardness measurements were made on the same transverse sections of the polished samples as we used for microstructure observations. Vickers microhardness was measured by applying 0.3 kg load for 10s by an Instron Tukon 2100 B Vickers hardness tester. An average of 10 readings of different indentations was taken for each sample.

3. Results and discussion

3.1. Effects of nickel on the microstructure of Sn-0.7Cu lead-free solders

Fig. 2 shows the effect of nickel on the microstructure of the tested Sn-0.7Cu solder alloy. The microstructure of the as-cast Sn-0.7Cu solder consisting of β-Sn dendrites and eutectic (β-Sn+Cu_6Sn_5) can be seen in Fig. 2a. Slightly any difference can be seen at a Ni level of 200 ppm (Fig. 2b). At the addition level of 400 ppm Ni, the volume fraction of eutectic (β-Sn+$(Cu,Ni)_6Sn_5$) is clearly higher than in the previous case (Fig. 2c), while the volume fraction of β-Sn dendrites is consistently lower. 800 ppm Ni content results in a fully eutectic microstructure without any primary phases (Fig. 2d). By 1800 ppm Ni doping, the microstructure becomes hypereutectic, consisting of primary $(Cu,Ni)_6Sn_5$ intermetallic phases, β-Sn dendrites (attributable to non-equilibrium solidification) and eutectic (β-Sn+$(Cu,Ni)_6Sn_5$) (Fig. 2e). These results are in good agreement with the literature, saying that Ni suppresses the formation of β-Sn dendrites in favour of the eutectic system [6-8]. With increasing nickel content, the microstructure changes from hypoeutectic through fully eutectic to hypereutectic.

TABLE 3

Chemical composition of the samples determined by ICP [wt.%]

Sample	Cu	Ni	Pb	Ag	As	Fe	Sb	Zn	Sn
Sn-0.7Cu	0.742	0.0005	0.0246	0.0148	0.0056	0.0161	0.0030	0.0011	bal.
Sn-0.7Cu-0.02Ni	0.737	0.0192	0.0246	0.0145	0.0046	0.0147	0.0025	0.0012	bal.
Sn-0.7Cu-0.04Ni	0.748	0.0383	0.0249	0.0178	0.0041	0.0188	0.0031	0.0026	bal.
Sn-0.7Cu-0.08Ni	0.752	0.0820	0.0252	0.0145	0.0038	0.0119	0.0039	0.0017	bal.
Sn-0.7Cu-0.18Ni	0.743	0.1779	0.0247	0.0143	0.0048	0.0170	0.0031	0.0024	bal.

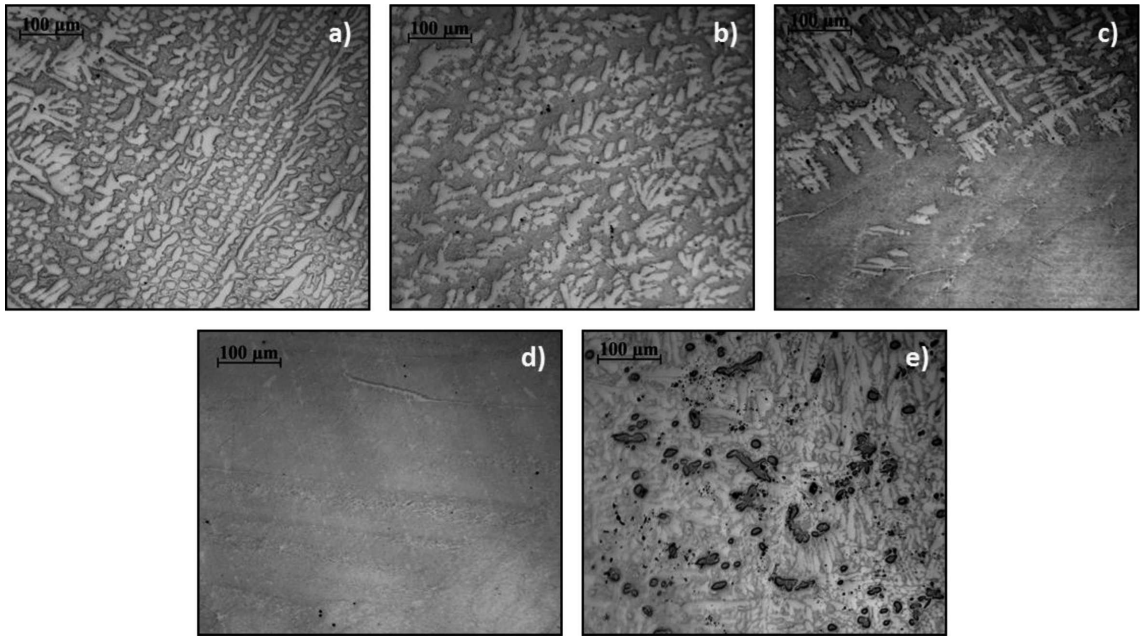

Fig. 2. Microstructural evolution of a Sn-0.7Cu solder from hypoeutectic (a,b,c) through fully eutectic (d) to hypereutectic (e) affected by Ni: a) 5 ppm Ni; b) 200 ppm Ni; c) 400 ppm Ni; d) 800 ppm Ni; e) 1800 ppm Ni

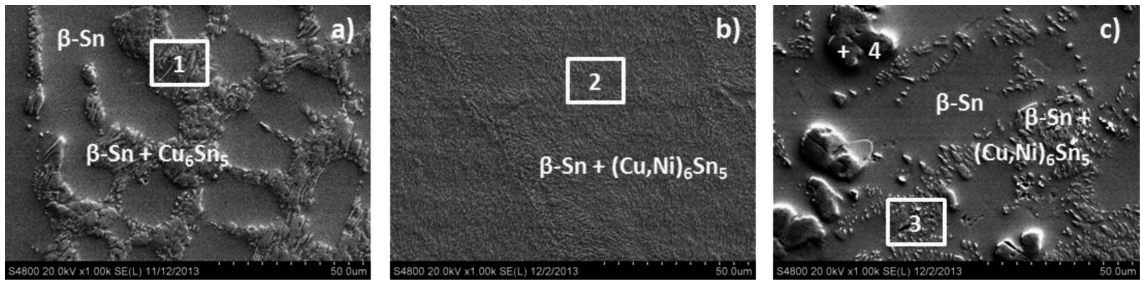

Fig. 3. SEM images of the examined solder alloys: a) Sn-0.7Cu; b) Sn-0.7Cu-0.08Ni; c) Sn-0.7Cu-0.18Ni

TABLE 4
Chemical composition of the analysed eutectic area and the primary $(Cu,Ni)_6Sn_5$ intermetallic phase of the examined samples shown in Fig. 3

Alloy	Analysed area()/point(+)	Analysed eutectic/phase	Chemical composition			
				Sn	Cu	Ni
Sn-0.7Cu	1	$Sn+Cu_6Sn_5$	wt.%	98.39	1.61	-
			at.%	97.04	2.96	-
Sn-0.7Cu-0.08Ni	2	$Sn+(Cu,Ni)_6Sn_5$	wt.%	99.40	0.56	0.05
			at.%	98.87	1.03	0.10
Sn-0.7Cu-0.18Ni	3	$Sn+(Cu,Ni)_6Sn_5$	wt.%	98.94	0.95	0.11
			at.%	98.02	1.75	0.22
Sn-0.7Cu-0.18Ni	4	$(Cu,Ni)_6Sn_5$	wt.%	66.44	24.50	9.07
			at.%	50.89	35.06	14.05

Fig. 3 shows the SEM images of Sn-0.7Cu (Fig. 3a), Sn-0.7Cu-0.08Ni (Fig. 3b) and Sn-0.7Cu-0.18Ni (Fig. 3c) alloys; TABLE 4 contains the chemical composition of the eutectics and the primary intermetallic phases. Since the Cu_6Sn_5 and $(Cu,Ni)_6Sn_5$ particles of the eutectic – particularly in the eutectic Sn-0.7Cu-0.08Ni alloy (Fig. 3b) – are very fine, they cannot be analysed with EDX, only an area analysis of the eutectic could be measured. The phases formed in Sn-0.7Cu-xNi solders are known from the literature, but the compositional determination of the intermetallics needs further investigation

by TEM. Based on the results of EDX analysis, the primary $(Cu,Ni)_6Sn_5$ intermetallic phase consists of 14 at.% Ni in the hypereutectic Sn-0.7Cu-0.18Ni alloy (Table 4), which corresponds to the reported data [8].

3.2. Effects of nickel on the mechanical properties of Sn-0.7Cu lead-free solders

Table 5 shows the mechanical properties of the examined solders. In Fig. 4, the effects of Ni on the tensile (UTS) and yield (YS) characteristics of a Sn-0.7Cu solder are presented, with magnified images of the microstructure. Figs. 5 and 6 show the effects of Ni on the elongation and microhardness (HV) of the Sn-0.7Cu solder.

TABLE 5
Mechanical properties of the examined solders with the standard deviations

Sample	UTS [MPa]	0.2YS [MPa]	Elongation [%]	HV
Sn-0.7Cu	30.25 ±3.19	23.55 ±1.99	32.18 ±4.89	10.7 ±0.4
Sn-0.7Cu-0.02Ni	32.27 ±2.73	24.29 ±1.45	32.44 ±11.65	11.7 ±0.4
Sn-0.7Cu-0.04Ni	36.72 ±1.33	27.65 ±2.03	28.56 ±5.05	13.2 ±0.8
Sn-0.7Cu-0.08Ni	43.09 ±2.83	33.19 ±3.10	18.75 ±3.38	15.2 ±0.7
Sn-0.7Cu-0.18Ni	28.17 ±1.18	20.33 ±0.94	33.29 ±8.18	10.2 ±0.5

As seen, nickel has a strong effect on the mechanical properties of the respective alloy, which is in good agreement with the results of the microstructural observations. As the nickel content increases UTS, YS (Fig. 4) and HV (Fig. 6) likewise increase up to a certain value. The Sn-0.7Cu solder reaches maximum strength at 800 ppm Ni, when the microstructure is fully eutectic. The appearance of large $(Cu,Ni)_6Sn_5$ intermetallic compounds in the microstructure causes a significant decrease in tensile strength, yield stress and microhardness. Elongation, however, is inversely affected by Ni addition (Fig. 5).

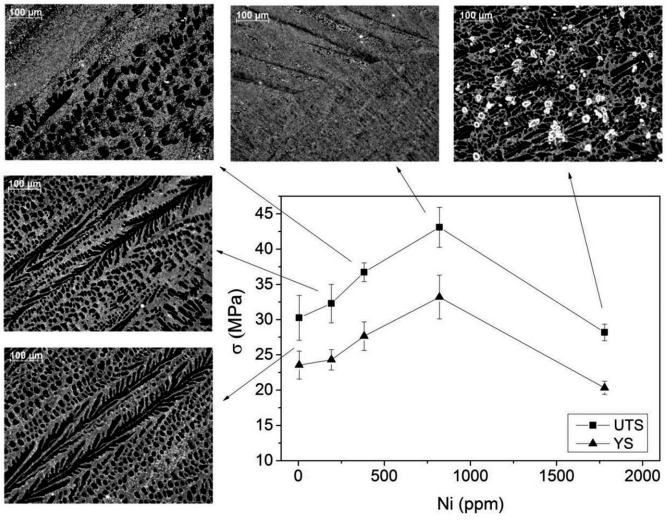

Fig. 4. Effects of nickel on the tensile properties and the microstructure of Sn-0.7Cu

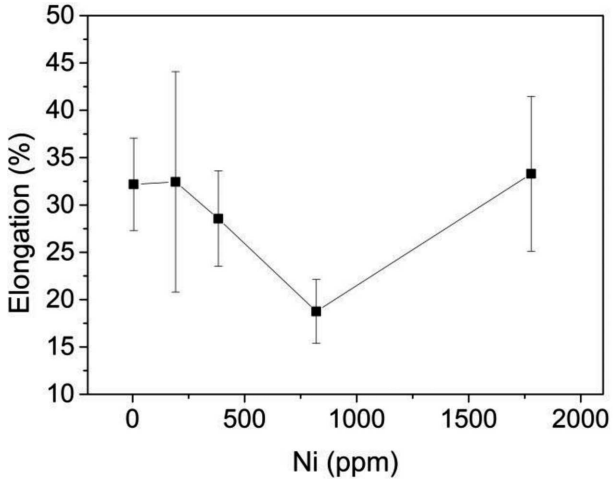

Fig. 5. Effect of nickel on the elongation of Sn-0.7Cu

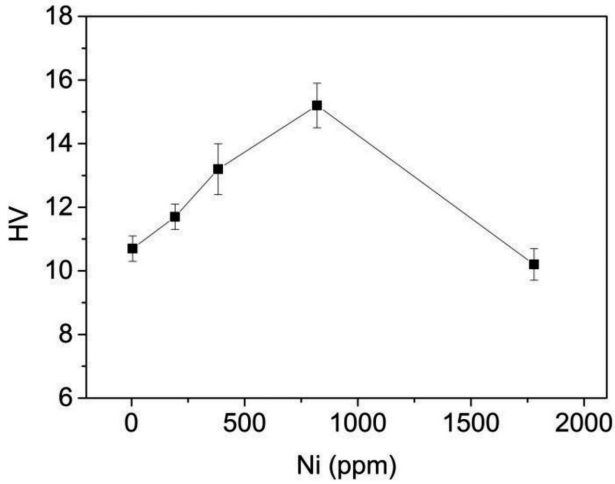

Fig. 6. Effect of nickel on the microhardness of Sn-0.7Cu

It is very important to avoid the formation of coarse primary $(Cu,Ni)_6Sn_5$ intermetallic compounds in the microstructure, lest they would lead to the mechanical deterioration and lifetime reduction of the solder joint. Furthermore, IMCs are likely to form bridges, causing short circuits during the wave soldering process [7]. Therefore, only eutectic or hypoeutectic (but close-to-eutectic) alloys can be applied in the soldering process. Given the results, under the present test conditions it is not recommended to add more than about 800 ppm Ni to the Sn-0.7Cu lead-free solder.

4. Conclusions

In this study, the effect of small amount of nickel addition (0, 200, 400, 800, 1800 ppm) on the microstructure and the mechanical properties of commercial purity Sn-0.7Cu lead-free solder alloys have been investigated. The relationships between microstructural evolution and mechanical property change are also described. The following conclusions can be drawn from the experimental results:

1. Increasing nickel content is directly associated with the microstructural evolution, from hypoeutectic through fully eutectic to hypereutectic, of Sn-0.7Cu lead-free

solders. The Sn-0.7Cu alloy becomes fully eutectic (β-Sn+$(Cu,Ni)_6Sn_5$) at 800 ppm Ni. Under the present experimental conditions, hypereutectic microstructure can be observed at higher Ni contents.

2. Nickel also strongly affects the mechanical properties of Sn-0.7Cu lead-free solders, basically due to the changes in the microstructure. The volume fraction of eutectic (β-Sn+$(Cu,Ni)_6Sn_5$) increases under the effect of Ni, which promotes the rise of tensile strength, yield stress, microhardness and the reduction of elongation. Maximum UTS, YS, HV and minimum elongation are achieved with 800 ppm of Ni addition (yielding a fully eutectic microstructure). Above this level, the UTS, YS and HV values decrease, while elongation significantly increases with the appearance of large primary $(Cu,Ni)_6Sn_5$ intermetallic compounds.

Acknowledgements

The authors would like to thank GLOB-Metal Kft. and Metalloglobus Zrt. for providing the solder alloys and the master alloy, dr. Olivér Bánhidi for the ICP measurements, dr. Mária Svéda Kissné for the SEM micrographs and the EDX analysis and Tamás Mikó for the tensile tests.

The research work presented in this paper is based on the results achieved within the TÁMOP-4.2.1.B-10/2/KONV-2010-0001 project and carried out as part of the TÁMOP-4.2.2.A-11/1/KONV-2012-0019 project in the framework of the New Széchenyi Plan. The realization of this project is supported by the European Union, and co-financed by the European Social Fund.

REFERENCES

[1] K.J. Puttlitz, K.A. Stalter, Handbook of lead-free solder technology for microelectronic assemblies, Marcel Dekker Inc., New York, 2004.

[2] H. Ma, J.C. Suhling, J Mater Sci. **44**, 1141-1158 (2009).

[3] G. Zeng, S. Xue, L. Zhang, L. Gao, J Mater Sci. **22**, 565-578 (2011).

[4] T. Ventura, S. Terzi, M. Rappaz, A.K. Dahle, Acta Mater. **59**, 1651-1658 (2011).

[5] I.T.L. Moura, C.L.M. Silva, N. Cheung, P.R. Goulart, A. Garcia, J.E. Spinelli, Mater Chem Phys. **132**, 203-209 (2012).

[6] T. Ventura, S. Terzi, M. Rappaz, A.K. Dahle, Acta Mater. **59**, 4197-4206 (2011).

[7] M. Felberbaum, T. Ventura, M. Rappaz, A.K. Dahle, JOM, 52-55 (2011).

[8] C.M. Gourlay, K. Nogita, A.K. Dahle, Y. Yamamoto, K. Uesugi, T. Nagira, M. Yoshiya, H. Yasuda, Acta Mater. **59**, 4043-4054 (2011).

[9] K. Nogita, Intermetallics **18**, 145-149 (2010).

[10] C.M. Gourlay, K. Nogita, J. Read, A.K. Dahle, J Electron Mater. **39**, 1, 56-69 (2010).

[11] C.M.L. Wu, D.Q. Yu, C.M.T. Law, L. Wang, J Electron Mater. **31**, 9, 928-932 (2002).

[12] C.M.L. Wu, M.L. Huang, J Electron Mater. **31**, 5, 442-448 (2002).

[13] S.-H. Huh, K.-S Kim, K. Suganuma, Mater Trans. **43**, 2, 239-245 (2002).

[14] http://www.boulder.nist.gov/div853/Publication%20files/NIST_ASM_Pb_free_casting.pdf

[15] A.A. El-Daly, A.E. Hammad, J Alloy Compd. **509**, 8554-8560 (2011).

[16] A.A. El-Daly, F. El-Tantawy, A.E. Hammad, M.S. Gaafarc, E.H. El-Mossalamy, A.A. Al-Ghamdi, J Alloy Compd. **509**, 7238-7246 (2011).

[17] J.H.L. Pang, Lead Free Solder: Mechanics and Reliability, Springer, New York 2012.

[18] S.D. Rani, G.S. Murthy, J Mater Eng Perform. **22**(8), 2359-2365 (2013).

[19] B.L. Silva, N. Cheung, A. Garcia, J.E. Spinelli, J Electron Mater. **42**, 1, 179-191 (2013).

[20] F. Zhu, H. Zhang, R. Guan, S. Liu, Microelectron Eng. **84**, 144-150 (2007).

[21] N. Bai, X. Chen, Z. Fange, J Electron Mater. **37**, 7, 1012-1019 (2008).

Received: 20 November 2014.